

# DISCRETE LINE SPECTROSCOPY AT THE EXTREMES OF ANGULAR MOMENTUM IN NORMAL DEFORMED $^{156}\text{Dy}$ AND GLOBAL DIFFERENTIAL LIFETIME MEASUREMENTS IN THE $A \sim 130$ HIGHLY-DEFORMED REGION\*

M.A. RILEY<sup>a</sup>, F.G. KONDEV<sup>a</sup>, A.V. AFANASJEV<sup>b†</sup>, T.B. BROWN<sup>a‡</sup>  
M.P. CARPENTER<sup>c</sup>, R.M. CLARK<sup>d</sup>, M. DEVLIN<sup>e</sup>, P. FALLON<sup>d</sup>, S.M. FISCHER<sup>c</sup>  
D.J. HARTLEY<sup>a§</sup>, I.M. HIBBERT<sup>f¶</sup>, R.V.F. JANSSENS<sup>c</sup>, D.T. JOSS<sup>g</sup>  
T.L. KHOO<sup>c</sup>, D.R. LAFOSSE<sup>e||</sup>, R.W. LAIRD<sup>a</sup>, T. LAURITSEN<sup>c</sup>, F. LERMA<sup>e</sup>  
M. LIVELY<sup>a</sup>, W.C. MA<sup>h</sup>, P.J. NOLAN<sup>g</sup>, N.J. O'BRIEN<sup>f</sup>, E.S. PAUL<sup>g</sup>  
J. PFOHL<sup>a</sup>, I. RAGNARSSON<sup>b</sup>, D.G. SARANTITES<sup>e</sup>, R.K. SHELINE<sup>a</sup>  
S.L. SHEPHERD<sup>g</sup>, J. SIMPSON<sup>i</sup> AND R. WADSWORTH<sup>f</sup>

<sup>a</sup> Dept. of Physics, Florida State University, Tallahassee, Florida 32306, USA

<sup>b</sup> Dept. of Mathematical Physics, Lund Institute of Technology, Lund, Sweden

<sup>c</sup> Physics Division, Argonne National Laboratory, Argonne, IL 60439, USA

<sup>d</sup> Nuclear Science Division, LBNL, Berkeley, California 94720, USA

<sup>e</sup> of Chemistry, Washington University, St. Louis, Missouri 63130, USA

<sup>f</sup> Dept. of Physics, University of York, York YO1 5DD, UK

<sup>g</sup> Oliver Lodge Laboratory, University of Liverpool, Liverpool L69 7ZE, UK

<sup>h</sup> Dept. of Physics, Mississippi State University, Starkville, MS 39762, USA

<sup>i</sup> CLRC, Daresbury Laboratory, Daresbury, Warrington, WA4 4AD, UK

*(Received January 13, 1999)*

The highest-spin discrete states ( $I \sim 60\hbar$  and  $E_x \sim 30\text{MeV}$ ) in normal deformed nuclei have been observed in the rare-earth isotope  $^{156}\text{Dy}$  using the GAMMASPHERE spectrometer. The quadrupole moments for a variety of configurations, including the  $9/2^+[404]$  ( $g_{9/2}$ ) proton,  $1/2^+[660]$  ( $i_{13/2}$ ) and  $1/2^-[541]$  ( $f_{7/2}, h_{9/2}$ ) neutron orbitals, were measured in a wide range of  $\sim 130$  nuclei.

PACS numbers: 23.20.Lv, 27.70.+q, 21.10.Re, 21.60.Ev

---

\* Presented at the XXXIII Zakopane School of Physics, Zakopane, Poland, September 1–9, 1998.

† Present address: Physik-Dept. T30, Tech. Univ. Munchen, D-85747 Munchen, DE.

‡ Present address: Chem. Dept., Univ. of Kentucky, Lexington, KY 40506, USA.

§ Present address: Dept. of Phys. and Astr., Univ. of Tennessee, Knoxville, TN 37996, USA.

¶ Present address: Oliver Lodge Lab., Univ. of Liverpool, Liverpool L69 7ZE, UK.

|| Present address: Dept. of Phys. and Astr., SUNY at Stony Brook, NY 11794, USA.

## 1. Introduction

The quest to observe increasingly high angular momentum states in atomic nuclei has helped drive the field of gamma-ray spectroscopy for many decades. Many surprising features have been discovered along the way and an ever blossoming variety of phenomena, exhibited by the nucleus as it builds up angular momentum, continues to be charted throughout the periodic table. It is in the rare-earth region near  $A \sim 150$ – $160$  that the highest spin discrete states in both normal deformed ( $I \geq 50\hbar$  [1, 2]) and superdeformed ( $I \geq 65\hbar$  [3]) nuclei have been discovered. We report the first observation of discrete levels with spin  $I = 60\hbar$  in a normal deformed nucleus,  $^{156}\text{Dy}$  [4], utilizing the high efficiency and resolving power of the Compton-suppressed Ge spectrometer array GAMMASPHERE [5], and discuss the competition between collective and terminating band structures at very high spin in  $N = 90$  nuclei.

The recent studies of highly deformed ( $\beta_2 = 0.3$ – $0.4$ ), sometimes referred to as “superdeformed”, structures in the region near mass  $A \sim 130$  have revealed an important interplay between microscopic shell effects, such as the occurrence of large gaps in the nucleon single-particle energies, and the occupation of high- $j$  low- $\Omega$  (intruder) orbitals in driving the nucleus towards higher deformation. Initially, it was thought that only the involvement of one or more  $i_{13/2}$  neutrons could result in a strong polarization on the nuclear shape in this mass region [6]. However, it was recently shown that bands built upon the  $9/2^+[404]$  ( $g_{9/2}$ ) proton orbital in the odd- $Z$   $^{131}\text{Pr}$  [7] and  $^{133}\text{Pm}$  [8] isotopes, exhibit quadrupole deformations comparable to the values found for highly deformed structures which include  $i_{13/2}$  neutrons. Furthermore, for nuclei below  $N = 73$  where the occupancy of the  $\nu i_{13/2}$  orbital is energetically unfavored, there are indications that bands involving the  $1/2^- [541]$  ( $f_{7/2}, h_{9/2}$ ) neutron may also be highly deformed [9, 10].

In order to elucidate the impact of the occupation of specific orbitals on the nuclear deformation, accurate lifetime measurements for a large number of bands in a variety of nuclei have been measured.

## 2. Discrete line spectroscopy in $^{156}\text{Dy}$ at the very highest spins

States at high spin and excitation energy in  $^{156}\text{Dy}$  were populated in the  $^{124}\text{Sn}(^{36}\text{S}, 4n)$  reaction using a 165 MeV beam from the 88'' Cyclotron at Lawrence Berkeley National Laboratory. The target consisted of two stacked  $400 \mu\text{g}/\text{cm}^2$  thick foils of  $^{124}\text{Sn}$ . The GAMMASPHERE array comprised 93 large-volume Compton-suppressed Ge detectors. A total of  $\sim 1.3 \times 10^9$  events were collected, when five or more Ge detectors were in prompt coincidence. The data were unfolded off-line into  $\sim 2.5 \times 10^{10} \gamma^3$  events and incremented into a number of RADWARE [11] cubes.

In  $^{156}\text{Dy}$ , more than thirteen sequences are observed beyond  $45\hbar$  with several near spin  $60\hbar$  [4]. For positive parity, the  $(+,0)_2$  and  $(+,0)_1$  bands are extended from  $I^\pi=36^+$  and  $46^+$  [1] to  $(62^+)$  and  $(58^+)$ , respectively. These are the highest spin discrete states observed to date in a normal deformed nucleus with the  $I^\pi=62^+$  state corresponding to an excitation energy of 30 MeV. The intensity of the highest observed transition being less than 0.02% of the reaction channel leading to  $^{156}\text{Dy}$ . For negative parity, the  $(-,0)_1$  band is extended from  $42^-$  up to  $52^-$ , but the  $(-,1)_1$  band is not extended, presumably because this structure terminates at the  $53^-$  state [1,4]. A similar termination effect also occurs for the  $(-,0)_1$  sequence at  $52^-$ .

The excitation energy of the (parity, signature)  $(+,0)$  bands in  $^{156}\text{Dy}$  observed to high spin are plotted with respect to a rigid rotor reference in Fig. 1. These structures are compared with the unpaired cranked Nilsson–

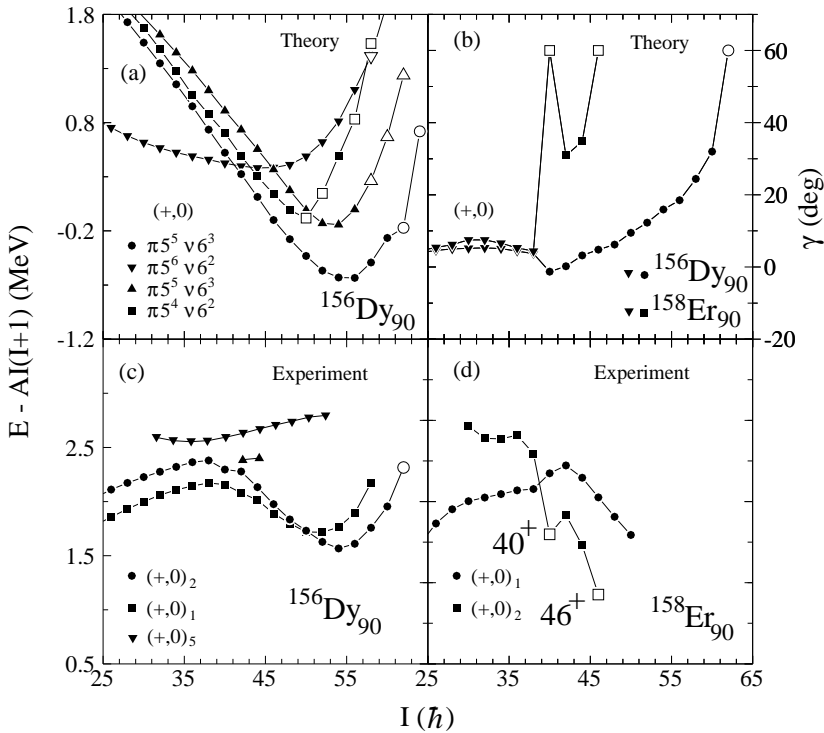


Fig. 1. (a) Calculated excitation energy minus a rigid rotor reference as a function of spin for the  $(+,0)$  bands in  $^{156}\text{Dy}$  [4]. (b) Calculated evolution with spin of the  $\gamma$  deformation for the yrast band in  $^{156}\text{Dy}$  and  $^{158}\text{Er}$ . (c) and (d) Experimental excitation energy of the  $(+,0)$  bands in  $^{156}\text{Dy}$  and  $^{158}\text{Er}$ , [4, 14].

Strutinsky calculations, similar to those described in reference [12]. The behavior of the highest spin states in the  $(+, 0)_1$  and  $(+, 0)_2$  bands is particularly interesting. These sequences begin to downslope above spin  $40\hbar$  where an “unpaired” band crossing occurs between competing structures [1], gaining energy with respect to the rigid rotor reference, but both display an upturn near  $I = 55$ . This is a characteristic of the phenomena of smooth, unfavored or soft band termination, typical in the  $A \sim 110$  mass region [13] but not previously seen in nuclei near  $A = 160$ . In soft band termination a particular configuration is followed through a long sequence of states and slowly evolves from a prolate collective ( $\gamma \sim 0^\circ$ ) shape to a fully aligned oblate ( $\gamma = 60^\circ$ ) shape. In general for this type of termination the state which has the maximum available spin for the configuration is high in energy and thus unfavored with respect to the rigid rotor, see Fig. 1. The comparisons between the calculations (Fig. 1(a)) and experiment (Fig. 1(c)) for  $^{156}\text{Dy}$  are particularly impressive. For example the calculations predict that the  $(+, 0)_2$  sequence may be associated with the  $\pi 5^5 \nu 6^3$  configuration. The calculations also predict [4] that the deformation of the  $(+, 0)_2$  sequence evolves smoothly with increasing spin from  $\varepsilon_2 \approx 0.19$ ,  $\gamma \sim 0^\circ$  at  $40^+$  (prolate) to  $\varepsilon_2 \approx 0.16$ ,  $\gamma \sim 16^\circ$  at  $54^+$  (triaxial), and finally to  $\varepsilon_2 = 0.10$ ,  $\gamma = 60^\circ$  for  $62^+$  (oblate) as shown in Fig. 1(b). The aligned state at  $62^+$  is associated with the configuration  $\pi[(h_{11/2})^5(g_{7/2}d_{5/2})^{-4}(d_{3/2})^1]_{29-} \otimes \nu[(i_{13/2})^3(h_{9/2}f_{7/2})^5]_{33-}$ .

The observation of unfavored band termination in  $^{156}\text{Dy}$  is in sharp contrast to the classic example of favored band termination in the neighboring  $N = 90$  nucleus  $^{158}\text{Er}$ , see Simpson *et al.* [14] and references therein, and Fig. 1(b) and 1(d) above. In  $^{158}\text{Er}$  the oblate terminating states are very favored and a rapid transition from prolate to oblate shape is observed along the yrast line. While the above data reveal compelling information regarding the energy behavior of the competition and evolution between collective and terminating structures in these  $N = 90$  nuclei, a complete understanding requires lifetimes of the states to be measured. While our results from a thick target experiment aimed at  $^{155}\text{Dy}$  have provided low statistic data on  $^{156}\text{Dy}$  which are consistent with the positive parity bands near  $I = 40$  being collective, a further more optimized study is needed to probe the highest spins in  $^{156}\text{Dy}$ . Also an experiment using the Cologne plunger with GAMMAS-PHERE has recently been performed on  $^{158}\text{Er}$  which will help elucidate the high spin behavior of this nucleus [15].

### 3. Differential quadrupole moment measurements in $A \sim 130$ highly deformed nuclei

While the quadrupole moment,  $Q_0$ , for some of the highly deformed bands in the  $A \sim 130$  region had been measured in the past using the

Doppler-shift attenuation method (DSAM), conclusive comparisons between different nuclei were limited owing to systematic distinctions between experimental setups such as varying reactions and target retardation properties. Specifically, due to differences in the parameterization of the nuclear and electronic stopping powers, which act as an “internal clock” in the DSAM lifetime measurements, large variations in the measured  $Q_0$  values have been reported for the same band. The absence of adequate experimental information on the time structure of the quasicontinuum sidefeeding contributions also results in an additional inaccuracy on the measured quadrupole moments. In the current work we have greatly reduced these systematic problems by measuring the lifetime decay properties of a large selection of bands in different nuclei under nearly identical experimental conditions in terms of angular momentum input, excitation energy and recoil velocity profile. Furthermore, the high efficiency and resolving power of GAMMASPHERE made it possible in favorable cases, to greatly minimize the effect of sidefeeding on the measured quadrupole deformations, by gating on shifted transitions at the top of the band of interest, thus gaining some insight into the nature and time scale of the sidefeeding.

High-spin states in a wide range ( $Z = 58\text{--}62$ ) of nuclei were populated after fusion of a  $^{35}\text{Cl}$  beam with  $^{105}\text{Pd}$  target nuclei. Thin and backed target experiments were performed at the 88-Inch Cyclotron at the Lawrence Berkeley National Laboratory with beam energies of 180 (thin target) and 173 MeV (backed target). The thin target consisted of an isotopically enriched  $^{105}\text{Pd}$  foil with a thickness of  $500\text{ }\mu\text{g}/\text{cm}^2$ . The backed target was a  $1\text{ mg}/\text{cm}^2$  thick  $^{105}\text{Pd}$  foil mounted on a  $17\text{ mg}/\text{cm}^2$  Au backing. Emitted  $\gamma$ -rays were collected using the GAMMASPHERE spectrometer [5] consisting of 57 (thin target) and 97 (backed target) HPGe detectors. The evaporated charged particles were identified with the MICROBALL detector system [16], whose selection capabilities allowed a clean separation of the different charged particle channels.

The present work focuses on the properties of structures which involve the important  $9/2^+[404]$  ( $g_{9/2}$ ) proton,  $1/2^+[660](i_{13/2})$  and  $1/2^-[541]$  ( $f_{7/2}, h_{9/2}$ ) neutron orbitals, in the odd- $N$  ( $Z = 60$ )  $^{133}\text{Nd}$  (populated in the  $\alpha\text{p}2\text{n}$  channel) and  $^{135}\text{Nd}$  ( $3\text{p}2\text{n}$ ) isotopes, and the odd- $Z$  ( $Z = 59$ )  $^{130}\text{Pr}$  ( $2\alpha 2\text{n}$ ),  $^{131}\text{Pr}$  ( $2\alpha 1\text{n}$ ) and  $^{132}\text{Pr}$  ( $1\alpha 2\text{p}2\text{n}$ ) nuclei. Typically more than about  $50 \times 10^6$  (thin target) and  $20 \times 10^6$  (backed target) events (of a fold  $\geq 3$ ) per particle gated channel were collected.

The backed target data were used to extract the quadrupole deformation using the centroid-shift technique in conjunction with the Doppler-shift attenuation method [17]. This was done in two ways. In the first method, the data were sorted into two-dimensional matrices in which one axis consisted of “forward” ( $31.7^\circ$  and  $37.4^\circ$ ) or “backward” ( $142.6^\circ$  and  $148.3^\circ$ ) group of

detectors and the other axis was any coincident detector. Spectra were generated by summing gates on the cleanest, fully stopped transitions at the bottom of the band of interest and projecting the events onto the “forward” and “backward” axes. These spectra were then used to extract the fraction of the full Doppler shift,  $F(\tau)$ , for transitions within the band of interest. In the second method, the data were sorted into a number of double-gated spectra which contained counts registered by particular group of detectors. Specifically, for the relatively strongly populated  $\nu i_{13/2}$  bands in  $^{133}\text{Nd}$  and  $^{135}\text{Nd}$ , gates were also set on in-band “moving” transitions in any ring of detectors and data were incremented into separate spectra for events detected at “forward”, “90°” and “backward” angles. Sample spectra for the  $\nu 1/2^+[660]$  ( $i_{13/2}$ ) band in  $^{133}\text{Nd}$  are shown in Fig. 2. It should be noted, that the implementation of the latter method made it possible to eliminate the effect of sidefeeding for states lower in the cascade.

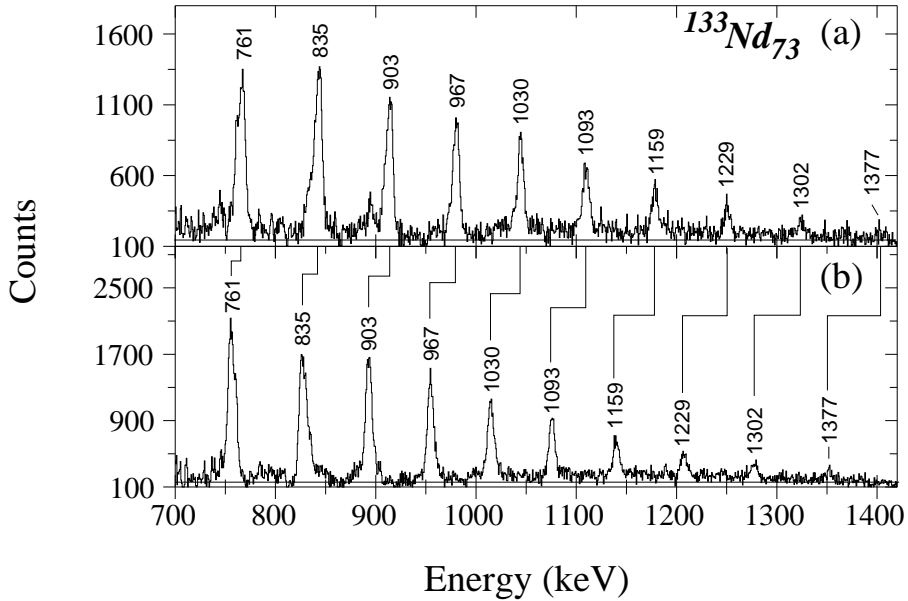


Fig. 2. (a) Forward and (b) backward angle coincidence  $\gamma$ -ray spectra [36] for the  $1/2^+[660]$  ( $i_{13/2}$ ) band in  $^{133}\text{Nd}$  formed from combinations of all double gates on in-band transitions from 345 keV up to 1228 keV. The peaks are labeled with the unshifted energies.

In order to extract the intrinsic quadrupole moments from the experimental  $F(\tau)$  values, calculations using the code FITFAU [19] were performed. The  $F(\tau)$  curves were generated under the assumption that the band has a constant  $Q_0$  value. In the modeling of the slowing process of

the recoiling nuclei, the stopping powers were calculated using the 1995 version of the code TRIM [20]. The corrections for multiple scattering were introduced using the prescription given by Blaugrund [21]. Where appropriate, the sidefeeding into each state was taken into account according to the experimental in-band intensity profile using a rotational cascade of three transitions with the same  $Q_0$  as the in-band states. It should be emphasized, that although the uncertainties in the stopping powers and the modeling of the sidefeeding may contribute an additional systematic error of 15–20% in the absolute  $Q_0$  values, the relative deformations are considered to be accurate to a level of 5–10%. Such precision allows a clear differentiation in the  $Q_0$  values to be made, which was used in turn as evidence for the involvement of specific orbitals within a band configuration.

### 3.1. Bands involving the $1/2^+[660]$ ( $i_{13/2}$ ) neutron orbital

Collective structures built upon the  $1/2^+[660]$  ( $i_{13/2}$ ) intruder neutron orbital have been observed in the chain of odd- $N$  ( $Z = 60$ ) Nd isotopes from  $^{133}\text{Nd}$  up to  $^{137}\text{Nd}$  [26, 27]. These bands have been connected to the normally deformed structures [27–32], so that their spin, parity and excitation energy are unambiguously determined. In addition, the  $g$ -factor experiment performed in the case of  $^{133}\text{Nd}$  [23] independently confirms the  $\nu 1/2^+[660]$  configuration assignment. Quadrupole moment measurements were carried out previously using both the centroid-shift and lineshape DSAM techniques [22–25, 33]. Lifetimes of low-spin members of the band in  $^{135}\text{Nd}$  and  $^{133}\text{Nd}$  were also measured via the Doppler-shift recoil-distance method [34, 35]. The  $F(\tau)$  values and the corresponding quadrupole deformations deduced in the current work when gates were set on the stopped 409, 440, 513 and 603 keV transitions in  $^{133}\text{Nd}$ , and 546 and 676 keV  $\gamma$ -rays in  $^{135}\text{Nd}$  are shown in Figs 3(c) and 3(d). Our observations (which are of higher precision) are in agreement with the previously measured quadrupole deformations for the bands in  $^{133}\text{Nd}$  [22], and  $^{135}\text{Nd}$  [24]. The comparison of the intensity profiles for these two bands, shown in Figs 3(a) and 3(b), reveals that the sequence in  $^{135}\text{Nd}$  is fed significantly from the side over a range of transitions for which the  $F(\tau)$  values change very rapidly. Such a behavior led to speculations [24, 25], that the sidefeeding lifetimes could be as much as four times slower than the in-band levels which led to the deduction of a quadrupole deformation for  $^{135}\text{Nd}$  which exceeded that of  $^{133}\text{Nd}$ . Figs 3(e) and 3(f) show our observations, when spectra gated on the Doppler-shifted in-band 1158, 1228, 1300 and 1377 keV  $\gamma$ -rays in  $^{133}\text{Nd}$ , and 1146, and 1216 keV  $\gamma$ -rays in  $^{135}\text{Nd}$ , were used. We found a roughly 10% increase in the deformation of both these two bands, compared to values deduced when gates were set on stopped transitions. These results allow us to estimate that the sidefeed-

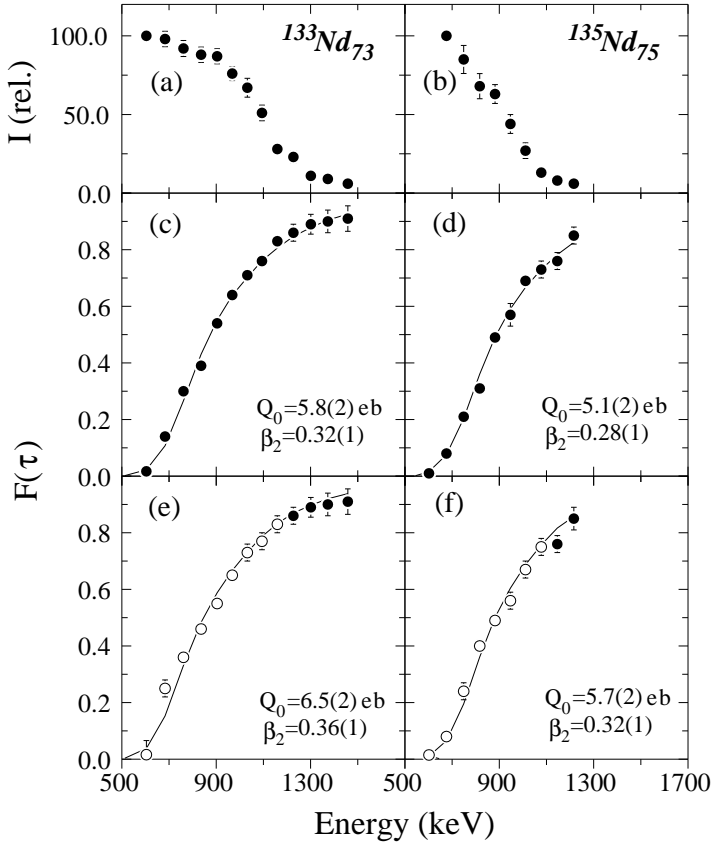


Fig. 3. Intensity profiles (a) and (b),  $F(\tau)$  values and corresponding quadrupole deformations deduced by gating on stopped transitions (c) and (d), and “moving” (solid) transitions (e) and (f) for the  $1/2^+[660]$  ( $i_{13/2}$ ) bands in  $^{133}\text{Nd}$  and  $^{135}\text{Nd}$ , respectively [36].

ing lifetimes are only about 1.3–1.4 times slower than those for the in-band levels which is consistent with recent measurements by Clark *et al.* [37] for superdeformed structures in  $^{131,132}\text{Ce}$ .

The present observations, together with the values for the band in  $^{137}\text{Nd}$  ( $Q_0=4.0(5)$  [ $\beta_2=0.22(3)$ ]) [22], indicate clearly for the first time that in the odd- $N$  Nd nuclei there is a systematic decrease in the deformation of the  $\nu i_{13/2}$  band as the neutron number increases [36]. Such an experimental trend is now in line with predictions by Total Routhian Surface and Ultimate Cranker calculations with pairing [22, 30], as well as by Cranked Nilsson–Strutinsky calculations [38] which do not include pairing.



### 3.2. Bands involving the $9/2^+[404]$ ( $g_{9/2}$ ) proton orbital

Initially, a highly deformed band built upon the  $9/2^+[404]$  ( $g_{9/2}$ ) proton orbital was observed in  $^{131}\text{Pr}$  by Galindo-Uribarri *et al.* [7]. The present work has established a value of  $Q_0 = 5.5(8)$  eb [ $\beta_2 = 0.32(5)$ ] for this band which is much larger than  $Q_0 = 3.9(3)$  eb [ $\beta_2 = 0.23(2)$ ] deduced for the normally deformed  $\pi h_{11/2}$  structure in the same nucleus. Recently, Brown *et al.* [39] have observed a strongly coupled band in the neighboring odd-odd  $^{130}\text{Pr}$  isotope which was suggested to include the  $9/2^+[404]$  ( $g_{9/2}$ ) proton orbital coupled to the  $7/2^- [523]$  ( $h_{11/2}$ ) neutron. The measured and calculated  $F(\tau)$  values for this structure, as well as those for the normally deformed  $\pi h_{11/2} \otimes \nu d_{5/2}$  band are shown in Fig. 4(a). The results for the  $\pi g_{9/2}$  and  $\pi h_{11/2}$  configurations in  $^{131}\text{Pr}$ , deduced from the current work, are presented in Fig. 4(b). We report  $Q_0 = 6.1(5)$  eb [ $\beta_2 = 0.35(3)$ ] for the  $\pi g_{9/2} \otimes \nu h_{11/2}$  band [40], which is similar or perhaps slightly larger compared to the value for the  $\pi g_{9/2}$  band in  $^{131}\text{Pr}$ . Our observations for the quadrupole deformations of the  $\pi g_{9/2}$  and  $\pi h_{11/2}$  bands in  $^{131}\text{Pr}$  are in agreement with

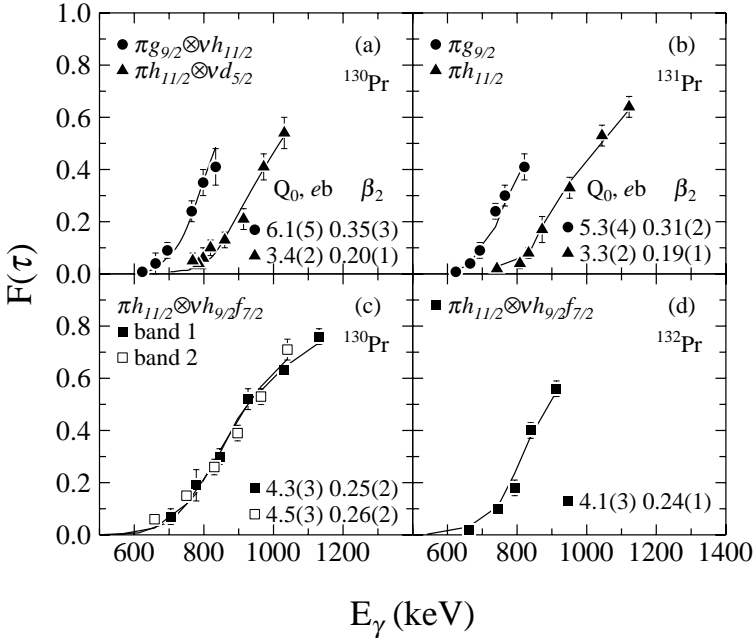


Fig. 4. The experimental and calculated  $F(\tau)$  values as a function of  $\gamma$ -ray energy for selected bands in  $^{130}\text{Pr}$ ,  $^{131}\text{Pr}$  and  $^{132}\text{Pr}$ . Calculated curves as shown as solid lines and correspond to the best fit to the data [40, 42].

the values reported by Galindo-Uribarri *et al.* [7]. It is notable that the deformation of structures that involve the  $\pi 9/2^+[404]$  ( $g_{9/2}$ ) configuration is comparable to those for the  $1/2^+[660]$  ( $i_{13/2}$ ) bands in the neighboring nuclei  $^{133}\text{Nd}$  and  $^{135}\text{Nd}$  isotopes thus confirming the important role played by the former orbital in building highly deformed structures in the region.

### 3.3. Bands involving the $1/2^-[541]$ ( $f_{7/2}, h_{9/2}$ ) neutron orbital

Two decoupled bands, referred to as band 1 and band 2 in the current work, were identified in  $^{130}\text{Pr}$  [41, 42] in agreement with the parallel work of Smith *et al.* [43]. We confirm the previously reported decoupled band in  $^{132}\text{Pr}$  [44, 45], but we propose different spin values compared to Ref. [45], and identify several additional in-band and inter-band transitions. These observations, together with the measured rotational alignments, band crossing properties and the orbitals expected near both the proton and neutron Fermi surfaces, led us to conclude that the configuration of these decoupled structures in  $^{130,132}\text{Pr}$  includes the  $1/2^-[541]$  ( $f_{7/2}, h_{9/2}$ ) neutron orbital coupled to the  $3/2^-[541]$  ( $h_{11/2}$ ) proton. Such an interpretation is also supported by the measured quadrupole deformations, shown in Figs 4(c) and (d). Thus, the occupancy of the  $1/2^-[541]$  ( $f_{7/2}, h_{9/2}$ ) neutron orbital results in the observation of enhanced deformed bands for nuclei below  $N = 73$ . The corresponding growth in quadrupole deformation values, however, is not as large as those observed when the  $\nu i_{13/2}$  or  $\pi g_{9/2}$  orbitals are involved.

## 4. Summary

The new generation of gamma-ray spectrometers, such as GAMMAS-PHERE, are now allowing us to perform exquisitely sensitive nuclear structure measurements. The first observation of discrete nuclear states at spin  $60\hbar$  in normal deformed nuclei were reported in  $^{156}\text{Dy}$ . Evidence for the positive parity yrast sequence experiencing an unpaired band crossing near  $I = 40\hbar$  and then evolving smoothly from a prolate (collective) shape towards an oblate (non-collective) shape at  $I \sim 60\hbar$  was presented. This result was contrasted with the well known sudden shape change observed in  $^{158}\text{Er}$ . In addition, the quadrupole moments of a number of bands, in several Nd and Pr nuclei, were measured using the Doppler-shift attenuation method as a part of our systematic study dedicated to understanding the properties of highly deformed structures in mass  $A \sim 130$  region. Differences in the observed deformations clearly demonstrate the important role played by the occupation of the  $9/2^+[404]$  ( $g_{9/2}$ ) proton,  $1/2^+[660]$  ( $i_{13/2}$ ) and  $1/2^-[541]$  ( $f_{7/2}, h_{9/2}$ ) neutron orbitals on the properties of the highly deformed bands.

The authors wish to thank the staff of the LBNL GAMMASPHERE facility and the crew of the 88" Cyclotron for their assistance during these experiments. The software support of D.C. Radford and H.Q. Jin and the target making wizardry of Bob Darlington are greatly appreciated. Support for this work was provided by the U.S. Department of Energy under Contract No. DE-AC03-765F00098 and Grant No. DE-FG02-88ER40406, the National Science Foundation, the State of Florida and the U.K. Engineering and Physical Sciences Research Council. MAR and JS acknowledge the receipt of a NATO Collaborative Research Grant.

## REFERENCES

- [1] J.D. Morrison *et al.*, *Europhys. Lett.* **6**, 493 (1988).
- [2] J. Simpson *et al.*, *J. Phys. G* **13**, L235 (1987).
- [3] S. Filbotte *et al.*, *Nucl. Phys.* **A584**, 373 (1995).
- [4] F.G. Kondev, *et al.*, *Phys. Lett.* **B437**, 35 (1998).
- [5] I.Y. Lee, *Nucl. Phys.* **A520**, 641c (1990); R.V.F. Janssens, F. Stephens, *Nucl. Phys. News*, **6**, 9 (1996).
- [6] R. Wyss *et al.*, *Phys. Lett.* **B215**, 211 (1988).
- [7] A. Galindo-Uribarri *et al.*, *Phys. Rev.* **C50**, (1994) R2655.
- [8] A. Galindo-Uribarri *et al.*, *Phys. Rev.* **C54**, 1057 (1996).
- [9] A. Galindo-Uribarri *et al.*, *Phys. Rev.* **C54**, R454 (1996).
- [10] R. Wadsworth *et al.*, *Nucl. Phys.* **A526**, 188 (1991).
- [11] D.C. Radford, *Nucl. Instrum. Methods Phys. Res.* **A361**, 297 (1995).
- [12] I. Ragnarsson *et al.*, *Phys. Scr.* **34**, 651 (1986).
- [13] I. Ragnarsson *et al.*, *Phys. Rev. Lett.* **74**, 3935 (1995).
- [14] J. Simpson *et al.*, *Phys. Lett.* **B327** (1994) 187.
- [15] S.L. Shepherd *et al.*, to be published.
- [16] D.G. Sarantites *et al.*, *Nucl. Instrum. Methods Phys. Res.* **A381**, (1996) 418.
- [17] T.K. Alexander, J.S. Forster, *Advances in Nuclear Physics*, New York: Plenum Press, vol.10, 1978, pp.197.
- [18] A.V. Afanasjev, I. Ragnarsson, *Nucl. Phys.* **A591**, 387 (1995).
- [19] E.F. Moore *et al.*, *Phys. Rev.* **C55**, R2150 (1997).
- [20] J.F. Ziegler, J.P. Biersack, U. Littmark, *The Stopping and Range of Ions in Solids*, New York: Pergamon Press, 1985; J.F. Ziegler, private communicate.
- [21] A.E. Blaugrund, *Nucl. Phys.* **88**, (1966) 501.
- [22] S.M. Mullins *et al.*, *Phys. Rev.* **C45**, 2683 (1992).
- [23] N.H. Medina *et al.*, *Nucl. Phys.* **A589**, 106 (1995).
- [24] R.M. Diamond *et al.*, *Phys. Rev.* **C41**, R1327 (1990).

- [25] C.M. Petrache *et al.*, *Phys. Rev.* **C57**, R10 (1998).
- [26] R. Wadsworth *et al.*, *J. Phys. G: Nucl. Phys.* **13**, L207 (1987).
- [27] E.M. Beck *et al.*, *Phys. Rev. Lett.* **58**, 2182 (1987).
- [28] D. Bazzacco *et al.*, *Phys. Lett.* **B309**, 235 (1993).
- [29] D. Bazzacco *et al.*, *Phys. Rev.* **C49**, R2281 (1994).
- [30] M.A. Deleplanque *et al.*, *Phys. Rev.* **C52**, R2302 (1995).
- [31] S. Lunardi *et al.*, *Phys. Rev.* **C52**, R6 (1995).
- [32] C.M. Petrache *et al.*, *Nucl. Phys.* **A617**, 228 (1997).
- [33] C.M. Petrache *et al.*, *Phys. Lett.* **B219**, 145 (1996).
- [34] P. Wilssau, *et al.*, *Phys. Rev.* **C48**, R494 (1993).
- [35] S.A. Forbes, *et al.*, *Z. Phys.* **A352**, 15 (1995).
- [36] F.G. Kondev *et al.*, *Phys. Rev. C*, submitted.
- [37] R.M. Clark *et al.*, *Phys. Rev. Lett.* **76**, 3510 (1996).
- [38] A.V. Afanasjev, I. Ragnarsson, *Nucl. Phys.* **A608**, (1996) 176.
- [39] T.B. Brown *et al.*, *Phys. Rev.* **C56**, R1210 (1997).
- [40] F.G. Kondev *et al.*, *Eur. Phys. J.* **A2**, 249 (1998).
- [41] F.G. Kondev *et al.*, *J. Phys. G.*, in press.
- [42] F.G. Kondev *et al.*, *Phys. Rev. C*, submitted.
- [43] B.H. Smith *et al.* to be published; L.L. Riedinger *et al.* private communicate.
- [44] K. Hauschild *et al.*, *Phys. Rev.* **C50**, 707 (1994).
- [45] S. Shi *et al.*, *Phys. Rev.* **C37**, 1478 (1988).